Image Pre-conditioning for Out-of-Focus Projector Blur

Michael S. Brown   Peng Song   Tat-Jen Cham

School of Computer Engineering

Nanyang Technological University, Singapore 639798

msbrown@ntu.edu.sg   psong@pmail.ntu.edu.sg   astjcham@ntu.edu.sg

Abstract

We present a technique to reduce image blur caused by out-of-focus regions in projected imagery. Unlike traditional restoration algorithms that operate on a blurred image to recover the original, the nature of our problem requires that the correction be applied to the original image before blurring. To accomplish this, a camera is used to estimate a series of spatially varying *point-spread-functions (PSF)* across the projector's image. These discrete *PSFs* are then used to guide a pre-processing algorithm based on Wiener filtering to condition the image before projection. Results show that using this technique can help ameliorate the visual effects from out-of-focus projector blur.

1. Introduction

Recent research focusing on projector-based displays has greatly increased the potential of light projectors as display devices. This is in part due to computer vision algorithms that couple projectors and cameras in the same environment. These so called *projector-camera systems* facilitate an array of applications, from the calibration of multi-projector display environments (see [4]), to techniques for user interaction [2, 3, 20], to algorithms for shadow correction and light suppression [5, 9] and even techniques for displaying on textured surfaces [14].

While significant advances to projector hardware have been demonstrated [13], on the whole, commodity projector hardware has not evolved to accommodate the flexibility allowed by projector-camera systems. Commodity light projectors are still designed to be used in an orthogonal (on-axis) manner with a planar display surface. While vision-based algorithms loosen these constraints and allow for more arbitrary positioning, one consequence is that of focus. Projectors' depth-of-field are often limited, and even slight off-axis projection can lead to blurred regions in the imagery. Currently, such blurred regions are simply ignored in lieu of the benefits obtained from flexible projector placement. Techniques to help reduce blur from focus, however, are undoubtedly welcomed.

Figure 1. (Left) Original image with blurring due to regions of the projected image being out-of-focus. (Right) The same image with our deblurring pre-conditioning.

[Our Contribution] We address the issue of out-of-focus projector blur. Our approach is formulated in the vein of traditional restoration algorithms focused on deblurring. Traditional approaches operate on a degraded image that has undergone some blurring process and try to approximate the original input image. Our problem is cast as the inverse – the original image is known, however, it cannot be processed once it undergoes the degradation process (i.e. projection). Thus, we need to pre-condition the image such that when projected the effects from out-of-focus blur will produce a result as close as possible to the original. To accomplish this, we have developed an algorithm that estimates the blurring process as a set of spatially varying *point spread functions* (PSFs) applied over the projected imagery. A pre-conditioned image is then computed from a set of Wiener filtered basis images computed from the estimated PSFs. Our results demonstrate that this procedure can help lessen the effects of blurring (figure 1 shows an example).

The remainder of this paper is as follows. Section 2 discusses related work; section 3 discusses background preliminaries to our approach; section 4 overviews our overall framework for computing the pre-conditioned image; section 5 shows results; section 6 and section 7 conclude with a discussion and summary of our work respectively.

2. Related Work

Research on camera-based algorithms for projector display and tiled display systems can be divided into two categories: (1) geometric calibration and (2) photometric calibration.

Geometric calibration algorithms use a camera (or cameras) to observe projected imagery to compute geometric transforms to rectify the imagery. These techniques can be used for problems as simple as key-stone correction, to calibration of multiple projectors over irregular surfaces. A number of papers have addressed geometric calibration for various setups and configurations [6, 15, 16, 17, 18, 21, 23]. Geometric correction can also be considered a pre-conditioning of the projected imagery, often referred to as *pre-warping*. In these approaches, the input image is warped before projection to compensate for projector positioning as well as the display surface geometry. The pre-warped image will appear geometrically correct when observed by a viewer. While pre-processing is applied to the displayed imagery it is only in the form of spatial transforms, the original image content is not modified.

Photometric algorithms use cameras to measure various photometric responses of the projectors. These approaches strive to create uniform (or perceptually uniform) imagery across a projector, or more often, across several overlapping projectors. These techniques are typically applied in tandem with geometric correction algorithms. Several papers have addressed this issue in various ways [10, 11, 12, 14, 17, 19]. Photometric correction can also be considered a pre-conditioning of the imagery. These techniques involve pixel-wise transforms to match colors or luminance values across the projectors and do not consider intensity spread due to blurring in the correction process.

In the context of image compositing, the issue of limited depth-of-field has been addressed (e.g. [1]). As previously mentioned, our projector-based problem is quite different: traditional approaches operate on the image after blurring; the nature of our problem requires that we process the image *before* the blurring occurs.

To our knowledge, no previous work has addressed the pre-processing of displayed imagery to offset image degradation due to blurring. In the following, we describe our framework and demonstrate the results of our image pre-conditioning algorithm on several testcases.

3. Preliminaries

3.1. Out-of-Focus Blur

When a projection setup is out of focus, the light rays emitting from a single projector pixel and collected by the lens system do not converge onto a single point on the display, but are instead distributed in a small area called the *circle-of-confusion*. A blurred image is caused not just by this dispersion of light but also the additive overlap of circles-of-confusion from neighboring pixels. The blur of an image depends on both the size of the circle-of-confusion as well as the distribution profile of light within it – this distribution of light is typically called the *point-spread function* (PSF). The PSF in turn depends on a number of factors including aperture size. Projectors and cameras typically do not have pinhole apertures and therefore have a finite depth-of-field. Projectors, in particular, are designed to have larger apertures that lead to brighter displays. Larger apertures however suffer from smaller depth-of-fields, *e.g.* in a thin-lens model the diameter of the circle-of-confusion for an out-of-focus point is directly proportional to aperture size. This is generally not a problem for projection systems as the projector is typically aligned orthogonal to a flat display surface, thereby allowing all points on the surface to be simultaneously in focus. However, in applications when the projector is significantly skewed to the display surface, or for substantially curved surfaces, there is only a small region on the display that is in sharp focus, while the other parts of the display suffer varying degrees of out-of-focus blur.

3.2. Uniform PSFs and Wiener Filtering

We initially consider the scenario in which a projector projecting orthogonally to a flat display surface is out of focus. In this setup, the display is uniformly blurred as the PSF (on the display) is reasonably invariant to the spatial position of the associated pixel in the image.

While the PSF depends on the lens system, it can be reasonably modeled as a 2D circular Gaussian [7] of the form

$$h_\sigma(x,y) = \frac{1}{2\pi\sigma^2} e^{-\frac{x^2+y^2}{2\sigma^2}}. \qquad (1)$$

The blurred image created from the overlap of the uniform PSF from different pixels can be modeled as the result of a convolution

$$\begin{aligned} i_B(x,y) &= i(x,y) \circ h(x,y) \\ &= \sum_u \sum_v i(x,y) h(u-x, v-y), \quad (2) \end{aligned}$$

where $i(x,y)$ and $i_B(x,y)$ are the original and blurred images respectively. Additionally, some additive noise may be present. In image processing, a typical problem is to recover the original but unknown image $i(x,y)$ given only the blurred image $i_B(x,y)$. If (2) is valid, the deblurring may also be achieved via convolution with an inverse filter $h^{-1}(x,y)$ such that

$$\begin{aligned} \hat{i}(x,y) &= i_B(x,y) \circ h^{-1}(x,y) \\ &= [i(x,y) \circ h(x,y)] \circ h^{-1}(x,y), \quad (3) \end{aligned}$$

where $\hat{i}(x, y)$ is the estimated deblurred image, assuming that $h^{-1}(x, y)$ exists and the noise is small.

In our problem, the sequence of operators is different. Here the goal is to *pre-condition* the known original image such that when it is displayed via the out-of-focus projector, the output image appears similar to the original image. Because convolution operators are commutative, (3) may be rewritten as

$$\hat{i}(x, y) = [i(x, y) \circ h^{-1}(x, y)] \circ h(x, y). \quad (4)$$

We can consider the pre-conditioned image to be the first term of (4), defined as

$$\tilde{i}(x, y) = [i(x, y) \circ h^{-1}(x, y)]. \quad (5)$$

Thus, the pre-conditioned image $\tilde{i}(x, y)$ after degradation $h(x, y)$ is an approximation of the original image $\hat{i}(x, y)$.

The challenge here is determining the optimal $h^{-1}(x, y)$, and this is easiest done in the frequency domain, where the blurring process may be dually treated as

$$I_B(u, v) = I(u, v)H(u, v), \quad (6)$$

where the $I_B(\cdot)$, $I(\cdot)$ and $H(\cdot)$ functions are Fourier transforms of the $i_B(\cdot)$, $i(\cdot)$ and $h(\cdot)$ functions respectively. If the PSF is known, a classical solution that minimizes the mean squared error is Wiener filtering (see [8]), for which a simple variation is:

$$\hat{I}(u, v) = \frac{H^*(u, v)I_B(u, v)}{|H(u, v)|^2 + 1/SNR}, \quad (7)$$

where $\hat{I}(\cdot)$ is the Fourier transform of $\hat{i}(\cdot)$, $H^*(\cdot)$ is the complex conjugate of $H(\cdot)$, and *SNR* is the estimated (or apriori) signal-to-noise ratio. Hence the pre-conditioning filter that is used for uniform PSF is simply given by

$$h^{-1}(x, y) = \mathcal{F}^{-1}\left\{\frac{H^*(u, v)}{|H(u, v)|^2 + 1/SNR}\right\}, \quad (8)$$

where $\mathcal{F}^{-1}$ is simply the inverse Fourier transform.

Considering (5), (7), and (8), it is apparent that the pre-condition image, $\tilde{i}(x, y)$ can be obtained by applying the Wiener filtering to the original image, $i(x, y)$, with H such that:

$$\mathcal{F}^{-1}\{\tilde{I}(u, v)\} = \mathcal{F}^{-1}\left\{\frac{H^*(u, v)I(u, v)}{|H(u, v)|^2 + 1/SNR}\right\}. \quad (9)$$

Assuming that the PSF is known or can be estimated from test images (*e.g.* fiducial markers), the Wiener filter allows for the pre-conditioning of images for out-of-focus projectors that are projecting orthogonally to the display surface.

3.3. Non-Uniform PSFs

When the projector is skewed to the display surface or for curved surfaces, the PSF is no uniform across the projector image. One significant consequence of this is that the convolution model no longer applies, and Wiener filtering cannot be directly used to pre-condition the image.

To address this problem, we estimate the spatially varying PSF profile across the projector. While we would like to estimate the PSF for each projector pixel, this is impractical in practice. As a compromise, we partition the projected image into smaller regions within which a PSF is computed. These sub-sampled PSFs are used to compute our pre-conditioned $\tilde{i}(x, y)$ by compositing a series of global PSF corrections described in the following section.

4. Framework For Image Pre-conditioning

4.1. Projector Blur Estimation

Our framework begins by estimating piecewise PSFs in the projector's image. The projector displays an image of equally sized feature markers (crosses) in an off-axis manner onto a flat surface. A high-resolution camera captures an image of these projected features. Since the displayed features and their observed locations in the camera are known, we can compute the 3×3 homography between the camera and display image to rectify the camera image to the original displayed image.

To derive the PSFs we would ideally compare the original image with the rectified camera image. These two images, however, are sufficiently different due to a variety of effects including the devices' imaging systems, display surface response, and properties such as the projector's lamp age and color balance settings. Given the difficulty in modeling (and estimating) these effects, we instead work directly from the rectified camera image. Our idea is to locate the most in-focus observed feature and use this rectified image as an *exemplar* for determining the PSFs of the other features. Since the camera image is rectified to the original projected image, the locations of the features are known. We use the notation $i_f(x, y)$ to denote the sub-image (bounding box) about a feature in the rectified camera image.

Due to lighting variations within the projector and illumination fall off from off-axis projection, intensity responses across the displayed image are not uniform. It is necessary to first normalize the features' intensities before finding the exemplar feature. In our setup, the illuminated display surface exhibits a reasonably uniform response to the projected light. As a result, we can exploit the nature of the PSFs to perform the intensity normalization. For display surfaces with non-uniform responses, more sophisticated illumination correction approaches can be used [12, 19].
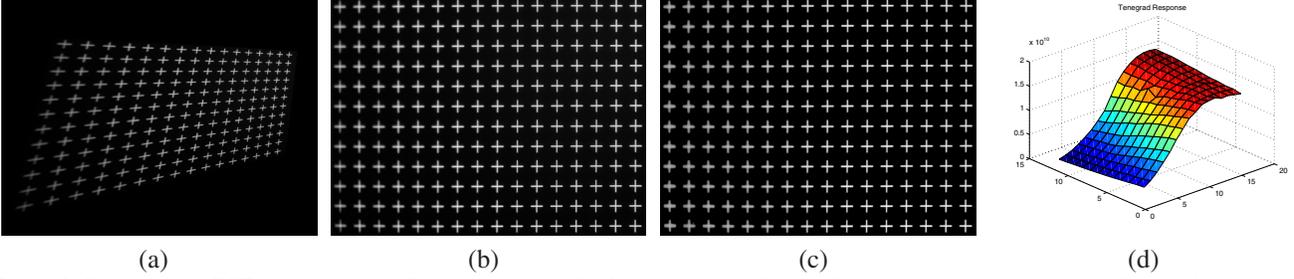
Figure 2. Stages of our PSF estimation. (a) Camera image of displayed features; (b) rectified image; (c) intensity normalized; (d) sharpness response for each feature.

The Gaussian PSF used in our blur model sums to unity and therefore does not change the overall energy of the original signal, *i.e.*, it does not change the DC component of the original $I(u, v)$. In other words:

$$I_B(0,0) = I(0,0)H(0,0) = I(0,0),$$

where the index $(0,0)$ represents the DC component of each I, I_B, and H functions in the Fourier domain. By finding the brightest feature $i_{max} = \max \sum_x \sum_y i_{f_j}(x,y)$, all other features, $i_{f_j}(x,y)$ can be normalized as

$$i_{f_j}(x,y) = \mathcal{F}^{-1}\{I_N(u,v)\}, \tag{10}$$

where

$$I_N(u,v) = \begin{cases} I_{max}(0,0) & \text{if } u = v = 0 \\ I_{f_j}(u,v) & \text{otherwise.} \end{cases}$$

From (10) we see that all features are now transformed to have the same DC component as the brightest feature.

After normalization, the sharpest feature in the image is found by computing a sharpness response in a block-wise fashion about each feature, $i_{f_j}(x,y)$, using the Tenengrad operator [22] as follows:

$$T_j = \frac{1}{n} \sum \mathbf{s}_x^2 + \mathbf{s}_y^2, \tag{11}$$

where, T_j is the sharpness response for feature $i_{f_j}(x,y)$, $\mathbf{s}_x$ and $\mathbf{s}_y$ are a 5×5 horizontal and vertical Sobel filter responses applied in the spatial domain over all n pixels composing the feature $i_{f_j}(x,y)$.

Figure 2 shows the steps to find the exemplar feature. Figure 2 (a) shows the original input image captured by the camera. This image is rectified to the projected image, figure 2 (b), and then normalized, figure 2 (c). Sharpness responses computed using (11) are obtained for each block as shown in figure 2 (d). Our exemplar feature, $i_e(x,y)$ is taken to be the feature corresponding to $\max(T_j)$.

4.1.1 PSF Map Recovery

Given the exemplar template, $i_e(x,y)$, we compute a set of k blurred templates with increasing σ, such that

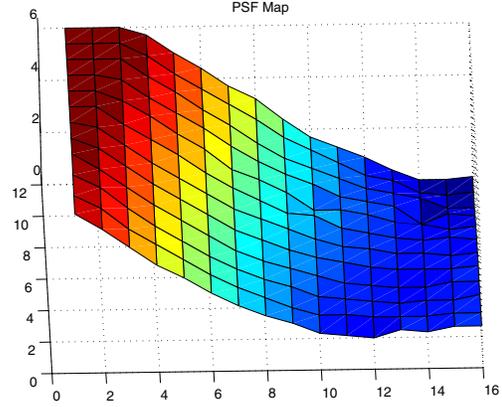$$i_{e(\sigma_k)}(x,y) = i_e(x,y) \circ h_{\sigma_k}(x,y),$$

Figure 3. Estimated PSF Map$_\sigma(u,v)$.

where $h_{\sigma_k}(x,y)$ represents the Gaussian PSF described in (1) with parameter σ_k. Typical values of $\sigma_k = \frac{1}{2}, 1, \frac{3}{2}, \cdots, 4$. These blurred $i_{e(\sigma_k)}(x,y)$ serve as templates for estimating the PSFs across the projector image. Cross correlation can be applied for each projected feature $i_{f_j}(x,y)$ against all blurred templates, $i_{e(\sigma_k)}(x,y)$, to find most similar $i_{e(\sigma_k)}(x,y)$ for each feature. Alternatively, we can also compute the Tenengrad response for each $i_{e(\sigma_k)}(x,y)$ and use this for matching PSFs, since the Tenengrad responses, T_j for each $i_{f_j}(x,y)$ are already available from the exemplar search.

The final result is a PSF map, $\text{Map}_\sigma(u,v)$ that assigns the appropriate σ_k to each feature $i_{f_j}(x,y)$ based on the template matching. Here we use (u,v) to represent the index of the sub-sampled feature [1]. The σ_k associated with each $\text{Map}_\sigma(u,v)$ corresponds to the PSF $h_{\sigma_k}(x,y)$ which best approximates the blurring in that region. Figure 3 shows the resulting $\text{Map}_\sigma(u,v)$. Not surprisingly, the shape of this map appears as the inverse of the Tenengrad responses.

---

[1]For simplicity in notation we reuse the variables (u,v), these should not be confused for the indices used for Fourier functions, *e.g.* $F(u,v)$.
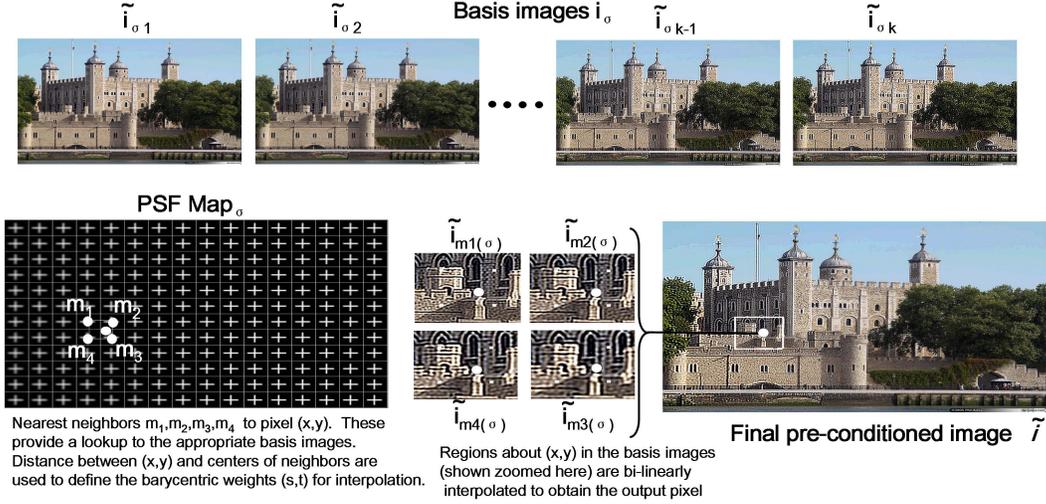
Figure 4. Piecewise PSF Filtering: (Top) Basis images $\tilde{i}_{\sigma_k}$. (Bottom-left) Shows PSF map and four nearest neighbors to pixel (x,y). (Bottom-middle) Shows zoomed in regions of four basis images. (Bottom-right) Final composited image.

4.2. Computing the Pre-conditioned Image

4.2.1 Basis Images via Wiener Filtering

As mentioned in section 3.3, because our PSFs are varying spatially within the image, Wiener filtering cannot be applied in a global manner to derive the pre-condition image $\tilde{i}(x, y)$. As a compromise, we approximate a spatially varying Wiener filter given the projector blur profile $\text{Map}_\sigma(u, v)$.

The $\text{Map}_\sigma(u, v)$ has k distinct PSFs defined as $h_{\sigma_k}(x, y)$. Using these $h_{\sigma_k}(x, y)$, we compute a set of preconditioned *basis images*, $\tilde{i}_{\sigma_k}(x,y)$, using Wiener filtering as described in (9), where the filter H for (9) is $\mathcal{F}\{h_{\sigma_k}(x, y)\}$. Figure 4 (top) shows an example of these basis images.

4.2.2 Image Compositing

For a given pixel in the pre-condition image, $\tilde{i}(x, y)$, we compute its value using a bi-linear interpolation of the basis images $\tilde{i}_{\sigma_k}(x, y)$. The appropriate basis images and weights for the interpolation are determined from the PSF $\text{Map}_\sigma(u, v)$.

Performing the appropriate coordinate scaling, we find the four closest neighbors in the PSF $\text{Map}_\sigma(u, v)$ to pixel (x, y). These four neighbors are denoted as $\mathbf{m_1}, \mathbf{m_2}, \mathbf{m_3}, \mathbf{m_4}$ and are ordered in a clockwise fashion about (x, y). Letting $\mathbf{m}(\sigma)$ refer to the $\mathbf{m}$'s corresponding

σ value, the interpolation is written as:

$$
\begin{aligned}
\tilde{i}(x, y) = {} & (1 - t)(1 - s)\, \tilde{i}_{\mathbf{m_1}(\sigma)}(x, y) \\
& + (1 - t)s\, \tilde{i}_{\mathbf{m_2}(\sigma)}(x, y) \\
& + ts\, \tilde{i}_{\mathbf{m_3}(\sigma)}(x, y) + t(1 - s)\, \tilde{i}_{\mathbf{m_4}(\sigma)}(x, y)
\end{aligned}
\tag{12}
$$

where s, $1 - s$, t, $1 - t$ are the appropriate barycentric coefficients, $(s, t \in [0..1])$, in the horizontal and vertical directions between the (x, y) location and the centers of the features associated with $\mathbf{m_1}, \mathbf{m_2}, \mathbf{m_3}, \mathbf{m_4}$. Performing this interpolation for each pixel we obtain the desired pre-conditioned image $\tilde{i}(x, y)$ needed for projection.

5. Results

Experiments are performed using a 3M MP8749 portable LCD projector with (1024×768) resolution, an Olympus C760 digital camera with 3.2M pixels and 10x optical zoom and a IBM Intellistation M Pro. The algorithms are all implemented in unoptimized Matlab 7.0 code.

For our experiments, we project a grid of 12×16 crosses. Features are bounded by 64×64 pixels blocks. Eight PSFs are estimated using $\sigma_k = \frac{1}{2}, 1, \frac{3}{2}, \cdots 4$ as discussed in Section 4.1.1. When computing the basis images, a SNR of 0.01 is provided in the Wiener filter to estimate noise present in the degradation process. Computation time, including estimating the PSFs, constructing the basis images, and compositing the final pre-condition image takes around 3-5 minutes.

We have selected test images that are sufficiently in focus and hope to demonstrate that results from our algorithm

are not merely attributed to a sharpening the input image. Please note that the pre-conditioned images will inherently appear sharper than the original, however, the original images themselves are sharp.

Figure 5 shows an example of our approach. Figure 5 (top-left) shows the original image of a "cat" and figure 5 (top-right) shows its appearance after projection. Note the out-of-focus blur appearing in the left-bottom corner. Figure 5 (bottom-left) is the corresponding pre-conditioned image $\tilde{i}(x, y)$ and its result, figure 5 (bottom-right), after projection. The texture of the cat's fur appears sharper in the pre-conditioned image (zoomed region). Figure 6 shows similar results for an outdoor scene. Again, our zoomed region show the pre-conditioned image appear sharper than the unprocessed image.

Figure 7 compares the results of our approach as an inset into the original projected image. Note that textures in the blurred regions are better preserved in the pre-conditioned image than the original.

Our results are subjective. Given the nature of the projector-camera system it is hard to compute quantitative results. As an effort to motivate our approach the following comparison is made. The error between the original image, i, and its blurred countered part, Blur(i), is computed. In this example, the blurring is synthesized using the same image compositing framework describe in section 4.2, except modified to produce basis images that are blurred based on the PSFs. We compare this error to the error between the original, i, and the pre-conditioned image under blur, Blur($\tilde{i}$). We show that we obtain $1 - 13\%$ improvement. The results are shown in the following table.

Figure	$\| i$-Blur(i)$\|$	$\| i$- Blur($\tilde{i}$) $\|$	Improvement
Colosseum (6)	22204	21030	+5%
Cat (5)	12217	12094	+1%
Temple (1 & 7.left)	20621	18163	+13%
Castle (7.right)	25806	23557	+9%

6. Discussion

6.1. Display Surface Geometry

In this paper, we focused solely on an off-axis projector to demonstrate our approach. In practice, our approach can be used with any display surface geometry. The only requirement is that the camera image of the displayed features be rectified back to the projector's coordinate frame. Several of the geometric calibration techniques (see [4]) provide methods for this rectification on non-planar surfaces.

6.2. Limitations

While the effects from projector blur cannot be completely remove, we have demonstrated that it is possible to pre-condition the image to lessen the effects. As with image restoration of blur, the effectiveness of our pre-conditioning approach is related to the estimation of the PSFs and input image itself. In the case of Gaussian PSFs, the Wiener procedure is effectively performing a sharpening. Input images which are already very sharp can result in noticeable ringing in the pre-conditioning process. Likewise, very large PSF (extreme blur) also result in over sharpening. We also note that it is possible that the pre-conditioning algorithm will result in pixel values outside the allowed intensity range of the graphics hardware and projector display capabilities. Research on ways to best deal with these issues warrants further investigation.

6.3. Spatial Sharpening

We initially examined approaches that applied spatial sharpening using an approximation of the inverse filter h^{-1} as specified in (8). To obtain acceptable results, however, we needed to use very large filters to the point where we were essentially performing the equivalent of the Wiener filter in the frequency domain using spatial convolution.

6.4. Future Work

While our Gaussian model is a reasonable approximation of projector blur, a formal investigation into image creation via projector systems and deeper analysis into projector specific PSFs is welcomed. As with many of the projector-camera systems research, our results are subjective. Providing results in the form of PSNR between input and displayed imagery is quite difficult for reasons discussed in this paper. A more systematic and formal approach for obtaining quantitative results between input and output image is needed.

7. Summary

A novel technique to pre-condition an image to counter the effects of image blurring due to out-of-focus regions in a projector has been presented. Our approach uses a camera image of the projected imagery to estimate the spatially varying PSFs across the projector image. A set of basis images are then constructed via Wiener filtering using the estimated PSFs. These basis images are compositied together based on projector's estimated blur profile to produce a pre-conditioned image. Our results demonstrate that displaying this pre-conditioned image is successful in lessening the effects of projector blur.

References

[1] M. Aggarwal and N. Ahuja. On generating seamless mosaics with large depth of field. In *ICPR*, pages 1588–1591, Barcelona, 2000.

[2] M. Ashdown and P. Robinson. Experiences implementing and using personal projected displays. In *PROCAMS*, Nice, France, 2003.
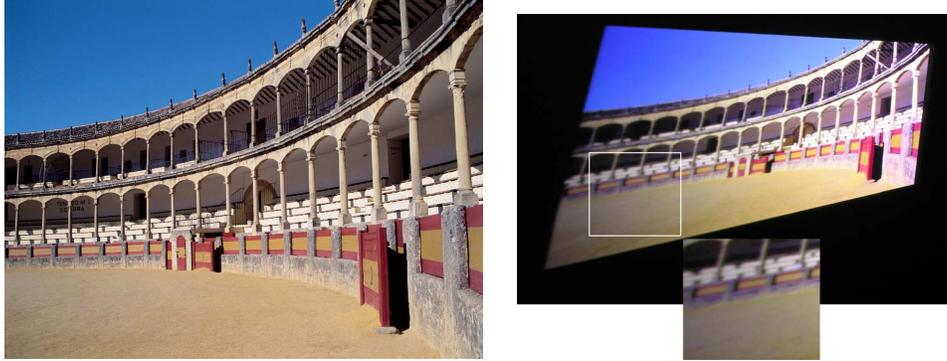
Original Image and Projection Result

Preconditioned Image and Projection Result

Figure 5. [Example 1] (Top) Original image and the results of its projection. (Bottom) Pre-condition image and the results of its projection. Note that textures are better preserved in the preconditioned image.

[3] D. Bandyopadhyay, R. Raskar, and H. Fuchs. Dynamic shader lamps: Painting on real objects. In *The Second IEEE and ACM International Symposium on Augmented Reality (ISAR'01)*, 2001.

[4] M.S. Brown, A. Majumder, and R.G. Yang. Camera-based calibration techniques for seamless multi-projector displays. *IEEE Trans. Visualization and Computer Graphics*, March 2005.

[5] T.J. Cham, J.M. Rehg, R. Sukthankar, and G. Sukthankar. Shadow elimination and occluder light suppression for multi-projector displays. In *CVPR'03*, Madison, WI, 2003.

[6] H. Chen, R. Sukthankar, G. Wallace, and K. Li. Scalable alignment of large-format multi-projector displays using camera homography trees. In *Proc. IEEE Visualization Conference*, Boston, MA, 2002.

[7] P. Favaro and S. Soatto. A geometric approach to shape from defocus. *PAMI*, 27(3):406–417, 2005.

[8] R. Gonzalez and R. Woods. *Digital Image Processing*. Addison-Wesley, 2nd edition, 2002.

[9] C. Jaynes, S. Webb, and R.M. Steele. Camera-based detection and removal of shadows from interactive multiprojector displays. *IEEE Trans. on Visualization and Computer Graphics*, 10(3):290–301, 2004.

[10] A. Majumder. Contrast enhancement of multi-displays using human contrast sensitivity. In *CVPR'05*, San Diego, CA, 2005.

[11] A. Majumder, Z. He, H. Towels, and G. Welch. Achieving color uniformity across multi-projector displays. In *Proc. IEEE Visualization Conference*, pages 117–124, Salt Lake City, UT, 2000.

[12] A. Majumder and R. Stevens. Color nonuniformity in projection-based displays: Analysis and solutions. *IEEE Trans. Visualization and Computer Graphics*, 10(2):177–188, 2004.

[13] S.K. Nayar, V. Branzoi, and T. Boult. Programmable image using a digital micromirror array. In *CVPR'04*, Washington, D.C., 2004.

[14] S.K. Nayar, H. Peri, M.D. Grossberg, and P.N. Belhumeur. A projection system with radiometric compensation for screen imperfections. In *PROCAMS*, Nice, France, 2003.

[15] T. Okatani and K. Deguchi. Autocalibration of projector-screen-camera system: Theory and algorithm for screen-to-camera homography estimation. In *ICCV'03*, pages 774–781, Nice, France, 2003.

[16] A. Raij, G. Gill, A. Majumder, H. Towles, and H. Fuchs. PixelFlex2: A comprehensive, automatic, casually-aligned multi-projector display. In *PROCAMS*, Nice, France, 2003.

Original Image and Projection Result

Pre-conditioned Image and Projection Result

Figure 6. [Example 2(Outdoor scene)] (Top) Original image and the results of its projection. (Bottom) Pre-condition image and the results of its projection. Note that textures are better preserved in the preconditioned image.

Figure 7. [Example 3] Inset of pre-condition image together with the original image. Note the difference in texture quality in the marked regions.

[17] R. Raskar, M.S. Brown, R.G. Yang, W.B. Seales, H. Towles, and H. Fuchs. Camera-registered multi-projector display on multi-planar surfaces. In *Proc. IEEE Visualization Conference*, San Francisco, CA, 1999.

[18] R. Raskar, G. Welch, M. Cutts, A. Lake, L. Stesin, and H. Fuchs. The office of the future : A unified approach to image-based modeling and spatially immersive displays. In *Proc. ACM SIGGRAPH*, Orlando, FL, 1998.

[19] P. Song and T.J. Cham. A theory for photometric self-calibration of multiple overlapping projectors and cameras. In *PROCAMS*, San Diego, CA, 2005.

[20] R. Sukthankar, R. Stockton, and M. Mullin. Smarter presentations: Exploiting homography in camera-projector systems. In *ICCV'01*, Vancouver, BC, 2001.

[21] R. Surati. *Scalable Self-Calibrating Display Technology for Seamless Large-Scale Displays*. PhD thesis, MIT, 1999.

[22] J.M. Tenenbaum. *Accommodation in Computer Vision*. PhD thesis, Standford, 1970.

[23] R. Yang, D. Gotz, J. Hensley, H. Towles, and M. S. Brown. Pixelflex: A reconfigurable multi-projector display system. In *Proc. IEEE Visualization Conference*, San Diego, CA, 2001.